Protoplasma (1992) 169: 28–41

PROTOPLASMA

Substructure of freeze-substituted plasmodesmata

B. Ding, R. Turgeon,** and **M. V. Parthasarathy***

Section of Plant Biology, Division of Biological Sciences, Cornell University, Ithaca, New York

Received October 11, 1991
Accepted February 29, 1992

Summary. The substructure of plasmodesmata in freeze-substituted tissues of developing leaves of the tobacco plant (*Nicotiana tabacum* L. var. Maryland Mammoth) was studied by high resolution electron microscopy and computer image enhancement techniques. Both the desmotubule wall and the inner leaflet of the plasmodesmatal plasma membrane are composed of regularly spaced electron-dense particles approximately 3 nm in diameter, presumably proteinaceous and embedded in lipid. The central rod of the desmotubule is also particulate. In plasmodesmata with central cavities, spoke-like extensions are present between the desmotubule and the plasma membrane in the central cavity region. The space between the desmotubule and the plasma membrane appears to be the major pathway for intercellular transport through plasmodesmata. This pathway may be tortuous and its dimensions could be regulated by interactions between desmotubule and plasma membrane particles.

Keywords: Freeze-substitution; High-pressure freezing; Intercellular transport; *Nicotiana tabacum*; Plasmodesmata; Propane-jet freezing.

Abbreviations: ER endoplasmic reticulum; PJF propane jet freezing; HPF high pressure freezing; CRT cathode ray tube; IP_3 inositol-trisphosphate.

Introduction

Plasmodesmata are cytoplasmic continuities between plant cells and they play potentially important roles in intercellular transport and signal transduction in plants (Gunning and Robards 1976, Robards and Lucas 1990). Several models of plasmodesmatal ultrastructure have been proposed (Lopez-Saez et al. 1966; Robards 1968, 1971; Zee 1969; Olesen 1979; Overall et al. 1982; Thomson and Aloia-Platt 1985; Olesen and Robards 1990; Tilney et al. 1991). There is now agreement that the plasma membrane of adjacent cells is continuous through the plasmodesmatal pores, that an axial component (desmotubule) runs through the pore and is in some way connected to, though not necessarily continuous with, the endoplasmic reticulum (ER), and that the two ends of the plasmodesma have constrictions at the "neck" region (see review by Robards and Lucas 1990).

Despite agreements on these points, some key issues of plasmodesmatal substructure remain unresolved. These include: the substructure and chemical composition of the desmotubule, the nature and size of particles within the cytoplasmic sleeve, and the existence or prevalence of a sphincter-like structure in the cell wall surrounding plasmodesmata.

Current knowledge of plasmodesmatal ultrastructure has been gained mainly from chemical-fixed or, in a few cases, freeze-fractured materials (see review by Robards and Lucas 1990). However, both techniques have drawbacks. Plasmodesmata have been shown to be dynamic entities (Baron-Epel et al. 1988); therefore the relatively slow penetration and mode of action of chemical fixatives may not lead to adequate preservation of the substructure of plasmodesmata. In addition, the fine structure of some cell components is known to be altered by chemical fixation; for example, the particulate nature of membrane proteins as revealed in many freeze-fracture micrographs is often obscured by glutaraldehyde fixation.

In the freeze-fracture techniques, the fracture plane occurs randomly and rarely exposes structures of interest. Moreover, replicas of freeze-fractured material are not very suitable for high resolution electron microscopy.

* Correspondence and reprints: Section of Plant Biology, Division of Biological Sciences, Cornell University, Ithaca, NY 14853, U.S.A.

** Present address: Department of Botany, University of California, Davis, California, U.S.A.

An alternate approach is to combine cryofixation and freeze-substitution techniques, which have been shown to yield superior preservation of even the very labile plant cytoskeletal elements, microfilaments, in addition to other cellular components (Lancelle et al. 1987; Tiwari et al. 1984; Tiwari and Polito 1988; Ding et al. 1991 b, c).

This paper presents an analysis of the substructure of plasmodesmata in tobacco leaves using freeze substitution techniques. Preliminary results were reported earlier (Ding et al. 1991 a).

Materials and methods

Plant material

Tobacco plants (*Nicotiana tabacum* L. var. Maryland Mammoth) were grown under greenhouse conditions as described in Ding et al. (1988). The plants used for experimentation were 8- to 10-weeks old. Leaves 12.0–13.0 cm in length were undergoing the sink-source transition (Turgeon 1987). The position of the import-termination boundary in the transition leaf was determined by transport experiments with $^{14}CO_2$-labeled photoassimilate (Turgeon 1987, Ding et al. 1988). Tissues from both the importing and nonimporting regions of the leaf were used for the plasmodesmatal structure study. Tissue in the nonimporting region was just starting to export photoassimilate.

Cryofixation and freeze-substitution

Tobacco leaf tissues from the importing part (basal) and the nonimporting part (tip) of four leaves were used for the study. Cryofixation and freeze substitution methods were the same as described by Ding et al. (1991 b). Briefly, a 2 × 2 cm leaf segment from the importing or nonimporting region of a developing leaf was first immersed in a 20 mM MES buffer solution (pH 5.5) containing 2 mM $CaCl_2$, 2 mM KCl and 0.2 M sucrose. The leaf segment was then aspirated gently for 1 min to remove intercellular air and thus facilitate buffer penetration. Samples of about 1 mm^2 containing class III veins (Ding et al. 1988) were dissected from the aspirated leaf segment under the buffer solution and were incubated in it for an additional 5 to 30 min. The samples were then frozen with a RMC MF7200 propane jet freezer (RMC, Tucson, Arizona), or a Balzers HPM010 high pressure freezer (Balzers Union, Liechtenstein). The buffer/sucrose treatment increased the depth of good freezing, but did not induce plasmolysis, cause other structural artifacts (Ding et al. 1991 b), or detectably perturb phloem loading or unloading (Turgeon 1984, 1987).

The frozen samples were freeze-substituted with 0.1% tannic acid in acetone at − 90 °C for two days, in 2% osmium tetroxide/2% uranyl acetate at − 20 °C for 1 day and at 4 °C overnight, and finally in pure acetone at 4 °C for 2 to 3 h. The samples were then warmed to room temperature, infiltrated with Spurr's resin (Spurr 1969), embedded, and polymerized.

In addition, some samples were freeze-substituted with 2% osmium tetroxide/2% uranyl acetate in acetone only and others were freeze-substituted with acetone alone. All treatments were done according to the time schedule given above.

Electron microscopy

A total of eight blocks, two blocks from each of the four leaves were used for analyzing plasmodesmata structure. Thin sections of 70 nm were cut with a diamond knife and stained with 2% uranyl acetate in 70% methanol and lead citrate. The sections were examined with a Hitachi H800 electron microscope operated at 150 kV. The electron microscope was equipped with an eucentric goniometer and a rotating specimen holder. Micrographs of both transverse and longitudinal views of plasmodesmata were taken at a series of tilt angles at 2° intervals ranging from + 24° to − 24°. In some cases, such serial-tilted micrographs were taken at every 45° rotation angle. All negatives were taken at × 120,000 magnification.

Computer image processing

A total of approximately 400 plasmodesmata from thin sections of the importing and the nonimporting tissues were analyzed under the electron microscope. Out of these about 100 were used for obtaining high resolution micrographs. From the micrographs obtained, 40 were selected (negatives or positives) for processing with a Tracor Northern TN8500 image processing system to enhance image contrast. The input into the image processor was through a Dage 68 series black/white high resolution video camera with a 1″ Newvicon tube. Both Kalman and exponential types of frame averaging of 100 frames each were done during acquisition and the digitized 512 × 512 pixel images (256 grey levels) were stored in the TN8500 system hard disk. Image enhancement was done by changing intensities of pixels in the recorded image to obtain the best contrast. The processed images were then transmitted to the high resolution CRT/camera of the H-800 transmission electron microscope (STEM) from which Polaroid type 55 positive/negative films were obtained.

Results

Figure 1 illustrates the general preservation quality of cell structures by freeze substitution. All organelles (Fig. 1 a) and cytoskeletal elements (Fig. 1 b) are well preserved. The plasma membrane is smooth and tightly appressed to the cell wall (Fig. 1 b). The image contrast of the ER is often low, as compared to other organelles such as mitochondria, plastids, and Golgi bodies. Both the propane jet freezing (PJF) and high pressure freezing (HPF) techniques preserve the substructure of plasmodesmata equally well.

We have examined plasmodesmata between various cell types in both the importing and nonimporting tissues of tobacco leaves. In importing tissue, plasmodesmata between most cell types are similar in structure. However, occasionally, plasmodesmata between bundle-sheath cells and phloem-parenchyma cells have central cavities (see Fig. 2). By contrast, in nonimporting tissue, all plasmodesmata contain central cavities (see Fig. 3 and 4). Central cavities in plasmodesmata therefore arise during leaf development. When central cavities are present, the two ends of the plasmodesmata remain unchanged, thus forming a "neck" region (see Fig. 2 c and d). Except for central cavities, no differences in

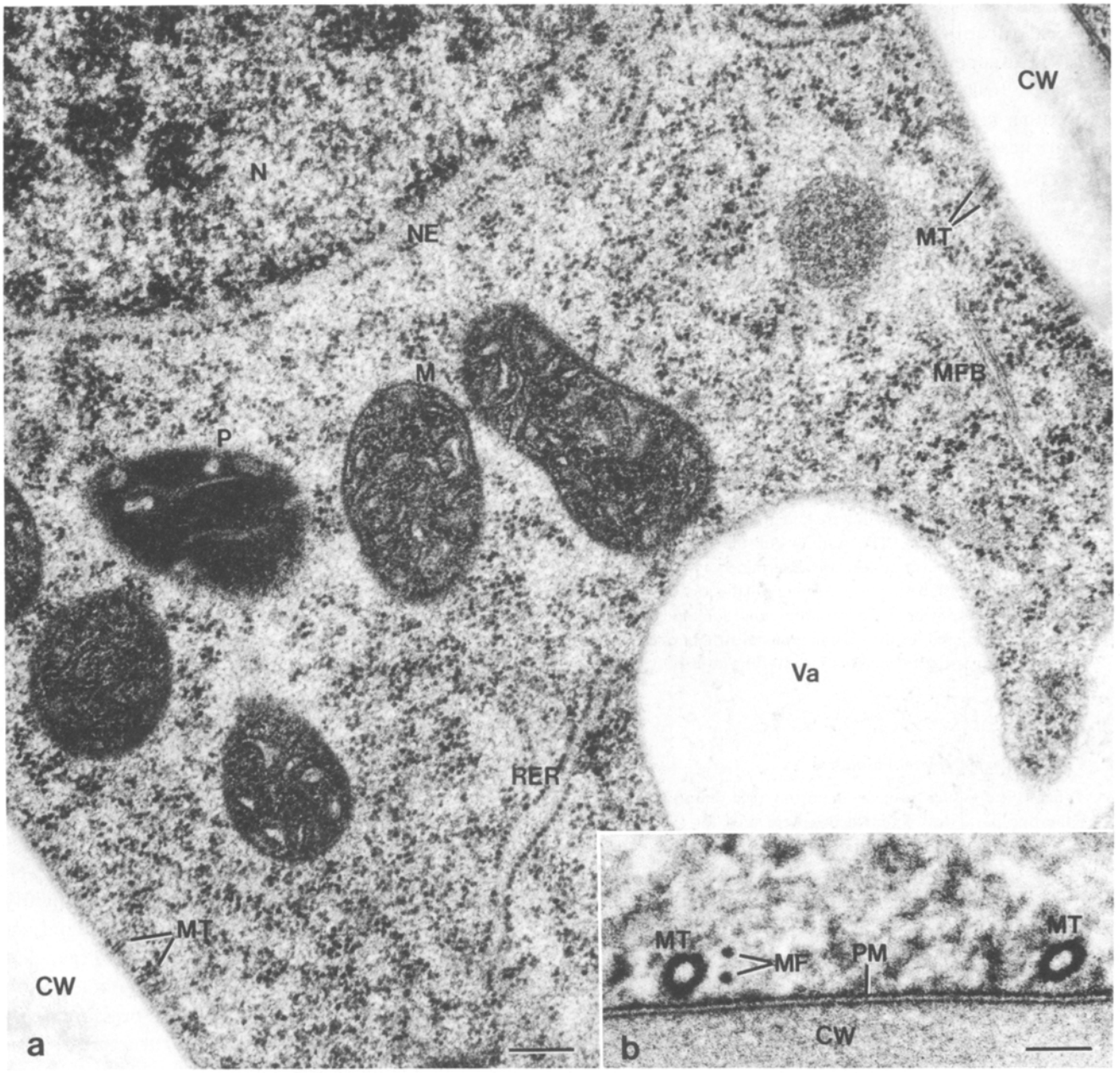

Fig. 1. Micrographs illustrating good preservation of cell ultrastructure after cryofixation. **a** A high pressure frozen companion cell. The plasma membrane is not clearly seen due to the oblique plane of the section. *CW* Cell wall; *M* mitochondrion; *MFB* microfilament bundle; *MT* microtubule; *N* nucleus; *NE* nuclear envelope; *RER* rough endoplasmic reticulum; *P* plastid; *Va* vacuole. Bar: 0.2 µm. **b** Microtubules (*MT*) in a mesophyll cell after HPF. Note that the plasma membrane (*PM*) is smooth and tightly appressed to the cell wall (*CW*). *MF* Microfilament. Bar: 40 nm

the structural features of plasmodesmata in importing and nonimporting tissues could be detected. For the results presented below, the terminology of Robards and Lucas (1990) for plasmodesmatal structure is followed.

Plasma membrane of plasmodesmata

The plasma membrane is continuous between adjacent cells through all plasmodesmata (Fig. 2). The inner leaflet of the plasma membrane (facing cytoplasm) of the

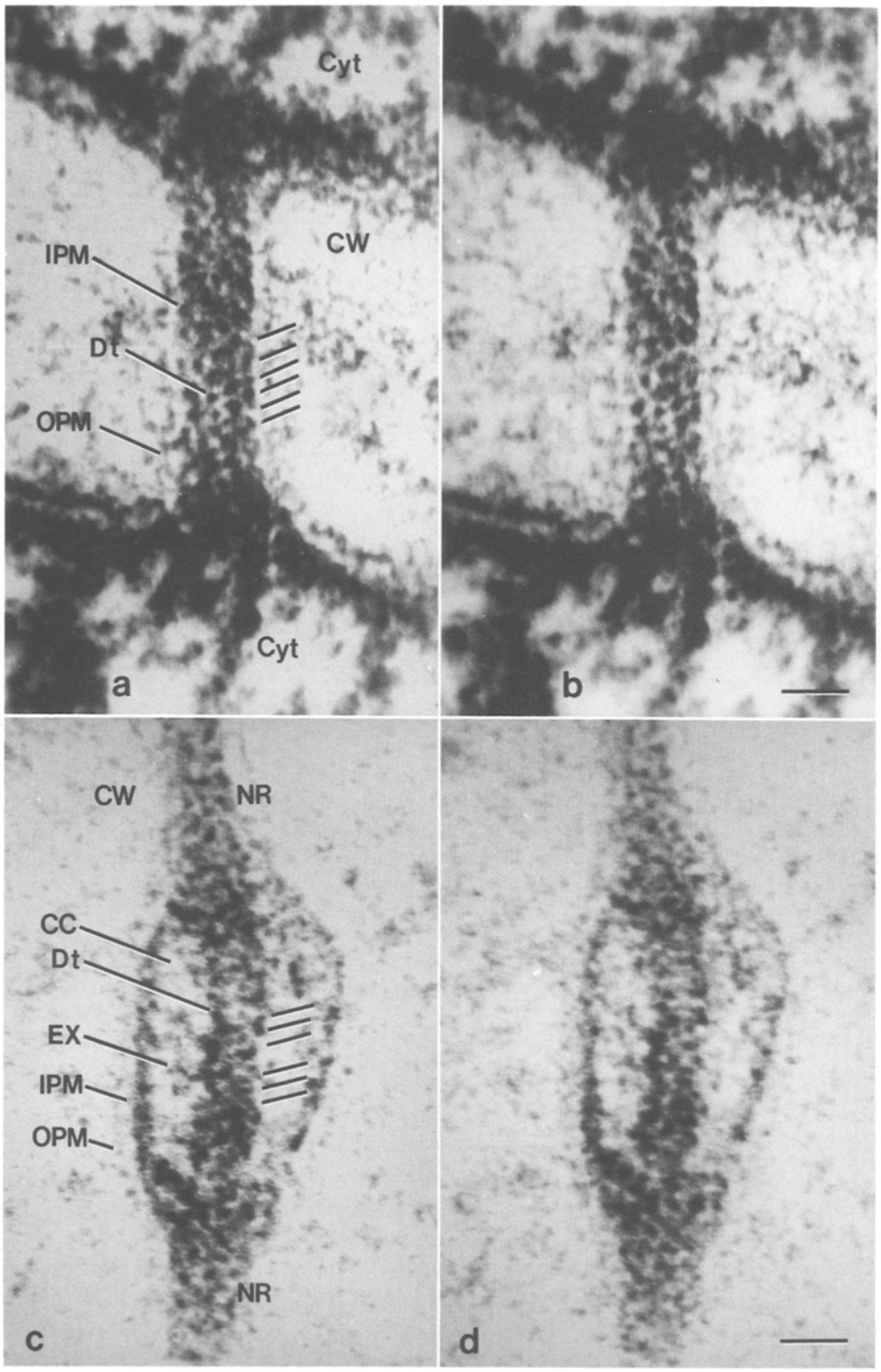

Fig. 2. Computer enhanced stereo pair-micrographs of longitudinal views of plasmodesmata. **a** and **b** A plasmodesma between phloem parenchyma cells of importing tissue. The parallel short lines indicate striations of particles of the desmotubule (*Dt*) and the inner leaflet of the plasma membrane (*IPM*). The outer leaflet of the plasma membrane (*OPM*) stains much more lightly than the inner leaflet. *CW* Cell wall; *Cyt* cytoplasm. HPF. Tilt angles: a, + 10°; b, + 8°. Bar: 18 nm. **c** and **d** A plasmodesma between a phloem parenchyma cell and a bundle sheath cell from importing tissue. The desmotubule (*Dt*) exhibits clear striations of particles which are indicated by short parallel lines. The inner leaflet of the plasma membrane (*IPM*) is much thicker than the outer leaflet (*OPM*). Note the presence of a central cavity (*CC*) and the unchanged two ends of plasmodesma that form the neck region (*NR*). Spoke-like extensions (*EX*) are present between the desmotubule and the plasma membrane in the central cavity. *CW* Cell wall. HPF. Tilt angles: c, − 6°; d, − 10°. Bar: 18 nm

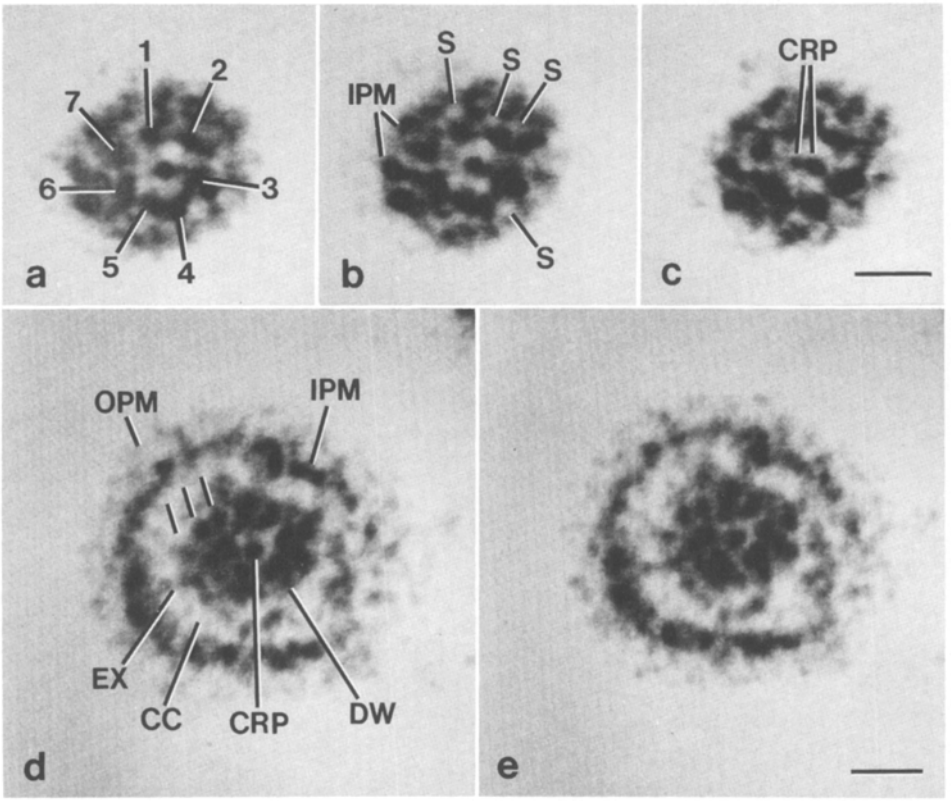

Fig. 3. Computer enhanced micrographs showing transverse views of plasmodesmata. **a–c** Neck region of a plasmodesma between phloem parenchyma cells of nonimporting tissue at various tilt angles. Since the computer enhancement is mainly set up to emphasize the particulate nature of plasmodesmata, low contrast images such as the outer leaflet of the plasma membrane are often lost during image processing. Note that the central rod particle (*CRP*) in **a** is resolved as two particles in **c** after progressive tilting. In **a**, the particles of the desmotubule wall are indicated numerically (*1–7*). In **b**, some of the spaces (*S*) (transport channels) between the particles of the desmotubule and the inner leaflet of the plasma membrane (*IPM*) are indicated. PJF. Tilt angles: a, − 10°; b, − 12°; c, − 16°. Bar: 11 nm. **d** and **e** The central cavity region (*CC*) of a plasmodesma between phloem parenchyma cells from nonimporting tissue. The desmotubule is probably curved (see Fig. 2 c and d), therefore an oblique view of the desmotubule wall (*DW*) reveals more than one layer of particles (short parallel lines). It is also possible that a proportion of the central cavity region is viewed along with the neck region to present such an image. *CRP* Central rod particle; *EX* spoke-like extension; *IPM* inner plasma membrane leaflet; *OPM* outer plasma membrane leaflet. PJF. Tilt angles: d, − 10°; e, − 12°. Bar: 13 nm

plasmodesmata is thicker than the outer leaflet (facing cell wall) (Fig. 2). This asymmetry is continuous along the entire length of a plasmodesma. In both longitudinal and transverse views, the inner leaflet of the plasma membrane contains electron-dense particles of about 3 nm diameter (Figs. 2 and 3; Table 1). This is especially evident in those plasmodesmata with central cavities (Figs. 2 and 3).

Desmotubule

A desmotubule is present in all plasmodesmata. In some plasmodesmata, the ER appears to be near, or perhaps in contact with, the desmotubule, as reported by many other authors (see review by Robards and Lucas 1990). However, this is not a consistent feature of plasmodesmata in our preparations. Due to the low contrast of ER, we cannot be certain that juxtaposed ER is absent in those cases where it was not visualized. Also, because of the low contrast of ER, we have been unable to determine whether there is continuity between the ER and the desmotubule in those cases where they are in close juxtaposition.

In transverse views, the desmotubule has a wall composed of 7 (but possibly more, see Discussion) electron-dense particles of about 3 nm diameter (Fig. 3 a and Table 1). In some oblique-transverse views, perhaps of curved desmotubules, the desmotubule wall particles appear to form striations (layers of rings) (Fig. 3 d and e). The presence of such layers of rings may also be due to a view that includes a proportion of the central cavity region along with the neck region. In longitu-

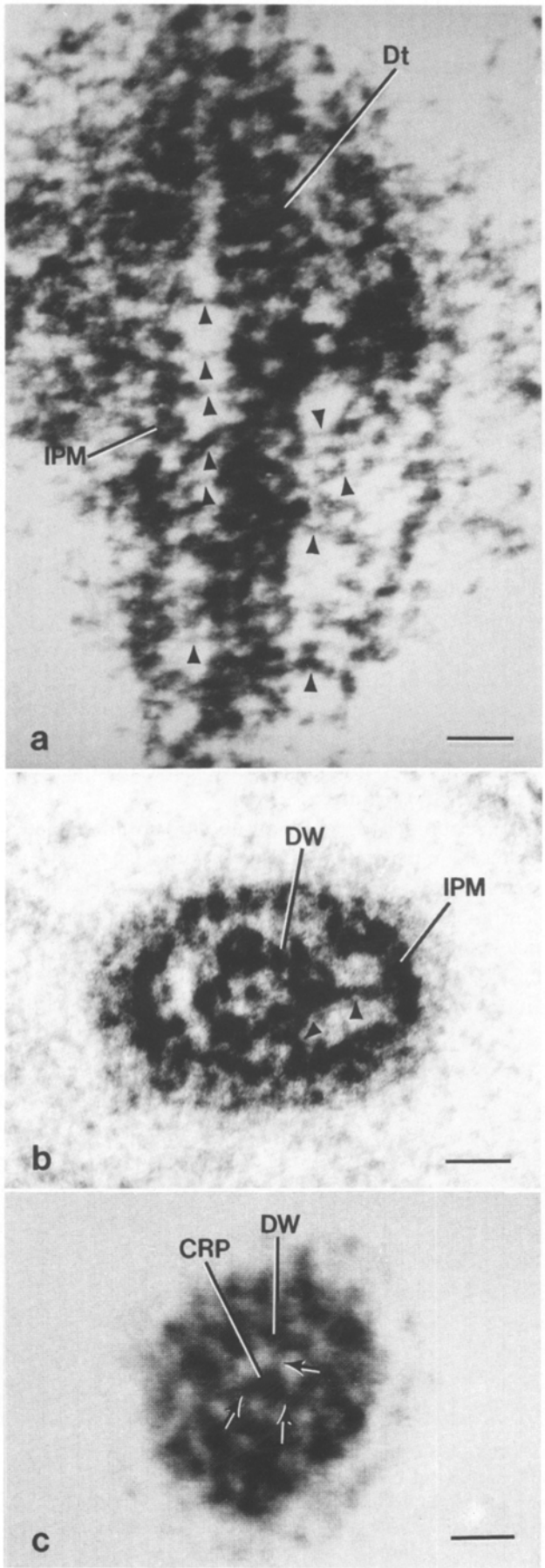

Fig. 4. Longitudinal and transverse views of plasmodesmata showing connections between components of plasmodesmata. **a** A computer-enhanced longitudinal view of the central cavity region of a plasmodesma, in which numerous spoke-like extensions (arrowheads) are present between the desmotubule (*Dt*) and the inner leaflet of the plasma membrane (*IPM*). Note the striated appearance of the desmotubule. Note also that the extensions seem to extend from desmotubule particles to plasma membrane particles. From phloem parenchyma cells after PJF. Bar: 13 nm. **b** A transverse view of a plasmodesma (not computer enhanced) between phloem parenchyma cells, showing spoke-like extensions (arrowheads) between the desmotubule wall (*DW*) and the inner leaflet of the plasma membrane (*IPM*). PJF. Bar: 12 nm. **c** A computer enhanced view of the neck region of a plasmodesma between phloem parenchyma cells, showing filamentous connections (arrows) between the central rod particle (*CRP*) and the desmotubule wall (*DW*). PJF. Bar: 7 nm

Table 1. Dimensions of particles and transport channels in plasmodesmata of tobacco leaves

Substructural component	Size (nm)	
	importing tissue	nonimporting tissue
Plasma membrane particle diameter	2.99 ± 0.36 (30)	2.83 ± 0.33 (27)
Desmotubule wall particle diameter	2.76 ± 0.27 (34)	2.77 ± 0.26 (28)
Center-center distance between desmotubule striations	3.89 ± 0.39 (11)	3.82 ± 0.36 (19)
Center-center distance between particles in a desmotubule striation	3.86 ± 0.33 (10)	3.90 ± 0.35 (13)
Central rod particle diameter	3.40 ± 0.40 (12)	3.20 ± 0.49 (8)
Presumed transport channel diameter (shaded area PTC in Fig. 7b)	2.49 ± 0.49 (37)[a]	2.28 ± 0.29 (26)[b]

For each substructural component, the numbers between the importing tissue and the nonimporting tissue do not differ (Mann-Whitney test, 95% confidence limit)

[a] Same value throughout the entire length of plasmodesmata

[b] For neck region only

dinal views, it is apparent that the entire length of the desmotubule is particulate (Figs. 2 and 4a). When the longitudinal sections are viewed at some tilt angles, the desmotubule particles appear to be arranged in a striated pattern, with 2 to 4 particles per striation (Figs. 2 and 4a). Such striated patterns are obscured and disappear after further tilt. While some desmotubules exhibit striations that are almost parallel to the transverse axis of the desmotubule, other striations are at an angle of up to 20–30° with reference to the transverse axis of the desmotubule (Figs. 2 and 4a). The center-to-center distance between the striations measures about 4 nm (Table 1). Within a striation, the distance between particles also measures about 4 nm (Table 1).

Tilney et al. (1991) have also reported "striations" along the plasmodesmata in the gametophytes of the fern *Onoclea sensibilis*, when tannic acid and ferric chloride are used in their fixation protocol. However, it is difficult to determine whether such striations are the same as those seen in tobacco desmotubules because of the relatively low magnification micrographs presented by those authors.

An electron-dense particle of about 3 nm in diameter is present in the center of the desmotubule in transverse views (Fig. 3 and Table 1). However, in some cases, the central particle of the desmotubule appears as two particles, when the section is progressively tilted (Fig. 3a–c).

In transverse sections cut at different planes along the

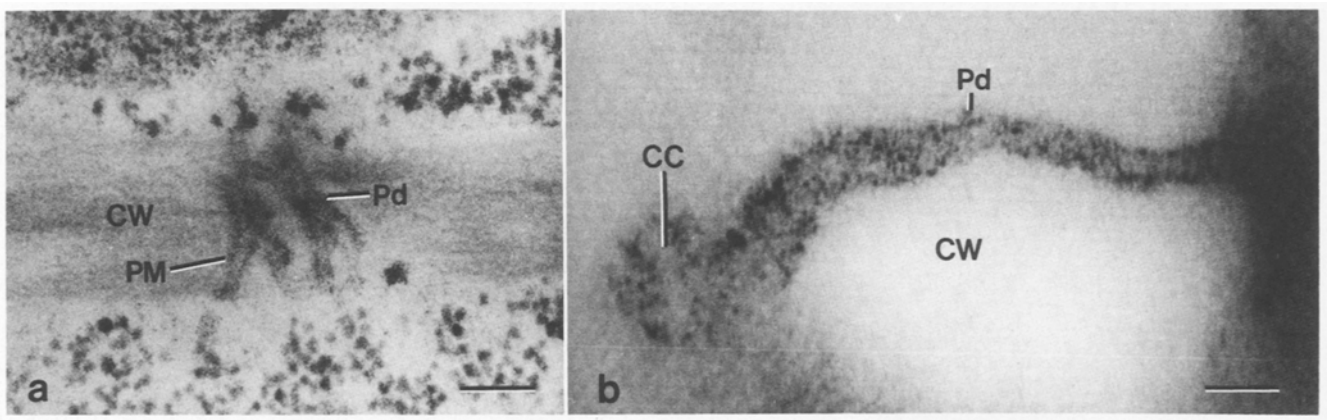

Fig. 5. Longitudinal views of plasmodesmata between phloem parenchyma cells freeze-substituted in acetone only. **a** The desmotubule of the plasmodesmata (*Pd*) is absent. The plasma membrane (*PM*) of the plasmodesmata is still present. In contrast, the plasma membrane lining the cell wall (*CW*) outside plasmodesmatal region is absent. PJF. Bar: 100 nm. **b** A computer enhanced high magnification view of a plasmodesma (*Pd*). Despite the presence of plasma membrane particles, most of the desmotubule particles are lost. This is particularly evident in the central cavity (*CC*) region. PJF. *CW* Cell wall. Bar: 42 nm

plasmodesmatal length, fine filamentous structures of about 1–1.5 nm in diameter are often seen extending from the central rod to the desmotubule wall (Fig. 4 c). In material freeze-substituted with acetone only, without tannic acid or uranyl acetate/osmium tetroxide, most of the desmotubule particles, including the central rod particles, are absent, though plasma membrane particles of plasmodesmata are still present (Fig. 5). It is noteworthy that although the plasma membrane particles of the plasmodesmata are present, the plasma membrane in other parts of the cell is completely removed by acetone (Fig. 5 a). This may indicate that the plasma membrane of plasmodesmata is specialized in some way.

Cytoplasmic sleeve

The cytoplasmic sleeve is the space between the plasma membrane and the desmotubule. In plasmodesmata without central cavities, the plasma membrane and the desmotubule are closely spaced together along their entire length (Fig. 2 a and b). Although it is a continuous structure, the cytoplasmic sleeve is not uniform in width due to the particulate nature of the desmotubule wall and plasma membrane. In transverse view, the irregular boundaries delimit 8–10 recognizable spaces, presumably transport channels, which are approximately 2.5 nm in diameter (see Fig. 6 a and Table 1). For easy visualization, one such channel is shown as a shaded area (PTC) in Fig. 7 b.

In plasmodesmata with central cavities, only in the neck region are the desmotubule and the plasma membrane in close alignment as described above (Fig. 2 c and d). In transverse views of the neck regions, spaces (transport channels) also of about 2.5 nm (Fig. 3 b and Table 1) in diameter are observed between the desmotubule and the plasma membrane particles. In the

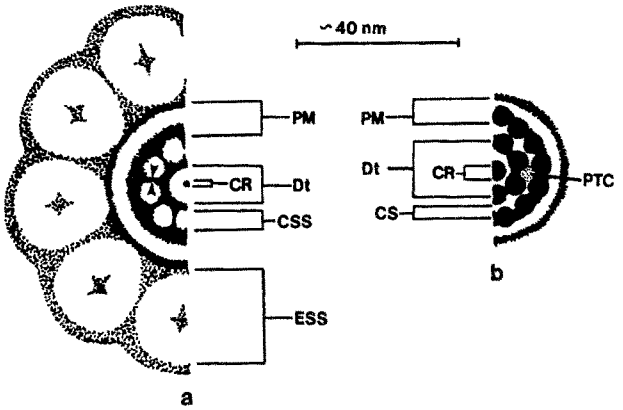

Fig. 7. A comparison between Olesen and Robards (1991) (**a**) and our interpretations (**b**) of plasmodesmatal structure (**a** is redrawn from Fig. 2 b of Robards and Lucas 1990). In **b**, there is no external sphincter subunits (*ESS*) as in **a**. The wall of the desmotubule (*Dt*) is an opaque ring in **a**, whereas in **b** it is particulate. The inner leaflet of the plasma membrane (*PM*) in **b** contains particles, in contrast to **a**. The cytoplasmic sleeve subunits (*CSS*) in **a** are interpreted as open spaces in the cytoplasmic sleeve (*CS*) in **b**. In **a**, the transport channels are assumed to be "gaps" between the "CSS" (indicated by arrowheads). In **b**, the presumed transport channels are spaces between the particles of the desmotubule and the plasma membrane. One of such channels is shaded and labeled as PTC. The dimension of these channels is given in Table 1

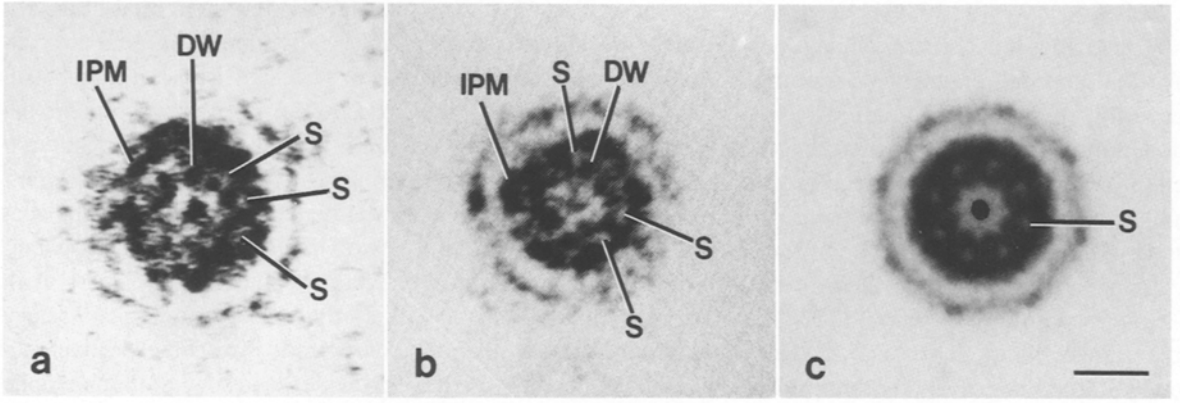

Fig. 6. Comparison of plasmodesmata in transverse views from an importing leaf tissue freeze-substituted with, and without, tannic acid. **a** A plasmodesma between mesophyll cells after freeze-substitution with tannic acid and uranyl acetate/osmium tetroxide in acetone. Note the spaces (*S*) between particles of the desmotubule wall (*DW*) and the inner leaflet of the plasma membrane (*IPM*). HPF. **b** A plasmodesma between phloem parenchyma cells freeze-substituted with uranyl acetate/osmium tetroxide in acetone only. Note similar spaces (*S*) between particles of the desmotubule wall (*DW*) and the inner leaflet of the plasma membrane (*IPM*), as in **a**. The central rod particles are not very distinct, presumably due to tilting effect. PJF. **c** A radially reinforced image of the cytoplasmic sleeve in **b**, using the technique of Markham et al. (1963). The spaces (*S*) between the desmotubule and the plasma membrane are reinforced, simulating eight "negatively stained particles" (see text for details on interpretation). The central rod region was blocked out during the reinforcement procedure. Bar: 11 nm

central cavity region, the desmotubule and the plasma membrane are widely separated and spoke-like extensions are present between them (Figs. 3 d, e and 4 a, b). The spoke-like extensions are absent in material freeze-substituted with acetone only. The widest part of the central cavity can reach a diameter of 30–40 nm.

Discussion

Tannic acid staining and interpretation of images

In reported studies of plasmodesmatal structure using chemical fixation, tannic acid of 1–2% has frequently been added to the primary fixative (Olesen 1979, Overall et al. 1982, Thomson and Platt-Aloia 1985, Tilney et al. 1991). Since tannic acid is known to stain microtubules negatively (Fujiwara and Linck 1982), a similar interpretation has often been made with reference to plasmodesmatal structure. In some cases the desmotubule is thought to be negatively stained (Robards 1968, Zee 1969, Olesen 1979, Tilney et al. 1991), and in others, "electron-lucent" (negatively stained) particles are identified in the cytoplasmic sleeve (between the desmotubule and the plasma membrane) (Overall et al. 1982, Thomson and Platt-Aloia 1985, Olesen and Robards 1990). In a recent model of plasmodesmata, the cytoplasmic sleeve is shown to be composed of 9 electronlucent subunits (Olesen and Robards 1990, Robards and Lucas 1990).

However, we contend that tannic acid does not negatively stain the plasmodesmata particles in freeze-substituted, and possibly also in chemically-fixed, materials. Our argument is based on the following considerations.

First, tannic acid does not stain all cellular components negatively. The concept of negative staining of macromolecules by tannic acid is mainly based on the observation and theory that, during tissue fixation and subsequent processing, tannic acid precipitates proteins and tannic acid-metal complexes are formed to shield protein macromolecules. Since the complexes scatter electrons strongly, the macromolecules appear to be in negative contrast (Futaesaku et al. 1972). However, while some cellular components such as microtubules are obviously stained negatively by tannic acid (Tilney et al. 1973), some are not; for example, microfilaments are stained positively (Seagull and Heath 1979, 1980; Ding et al. 1991 c). Therefore, the type of staining pattern created by tannic acid depends on the chemical nature of the cellular component in question, although the details of the staining mechanism are not understood. A simple extrapolation of the negative staining effect of tannic acid on some structures to plasmodesmata (Olesen 1979, Overall et al. 1982, Tilney et al. 1991) is thus not safely warranted.

Second, in tissues processed with and without tannic acid, the staining patterns of plasmodesmata are the same. Our Fig. 6. a and b compares plasmodesmata from tissues freeze-substituted with tannic acid and osmium tetroxide/uranyl acetate and those freeze-substituted with osmium tetroxide/uranyl acetate alone. It shows that tannic acid helps to preserve plasmodesmatal particles better, but does not stain them negatively. A comparison of Fig. 13 (without tannic acid in the primary fixative) and Fig. 14 (with tannic acid in the primary fixative) in Overall et al. (1982) demonstrates that the staining patterns of plasmodesmata are also the same, and not reversed, in the two treatments. In fact, without tannic acid staining, the particulate nature of the desmotubule is apparent in Fig. 13 of Overall et al. (1982). However, the same authors have pointed out that the similarity between the images obtained with and without tannic acid could be due to natural tannins in the vacuole released during chemical fixation. Tobacco leaf tissues are known to have phenols with one o-dihydroxyl group in the aromatic ring that reacts with osmium-iodide mixtures to produce brilliant staining of phenol-containing vacuoles, at the light microscopy level. However, phenols containing only one hydroxyl group or m-dihydroxy groups fail to react quickly and/or form black products when treated with osmium-iodide mixtures (Scalet et al. 1989). Another factor to be considered is that the amount of phenols present is often related to the type of organ, the tissue and its developmental stage. In chemically fixed (Ding et al. 1988) as well as in cryofixed/freeze-substituted tobacco leaves (Ding et al. 1991 b), a flocculent material is often present in the vacuole. We do not know whether the vacuolar material is a phenolic compound. However, it is quite different in appearance from the dense material filling the vacuoles in some species of *Azolla* that have been chemically fixed without tannic acid (e.g., Calvert et al. 1986). Thus it is likely that tobacco and *Azolla* have different phenolic compounds in their respective vacuoles. We also have no evidence to suggest that phenolic compounds that may be in the vacuoles leak into the cytoplasm during chemical fixation of the tobacco leaf, since there is no difference in the vacuolar contents between cryofixed/freeze-substituted and chemically fixed cells.

Third, tannic acid overstaining can produce spurious images that appear to be negatively stained. As dis-

cussed by Fujiwara and Linck (1982), it is extremely important to use tannic acid of low-molecular weight and at low concentrations. A concentration of more than 1% can result in extensive precipitation inside and outside the cell, and this can obscure fine cell structure (Fujiwara and Linck 1982). For example, the normal diameter of microfilaments (6–7 nm) is increased to 13 nm by the use of 1% tannic acid (Seagull and Heath 1979). Figure 14 in Overall et al. (1982) shows that the plasma membrane and the desmotubule are very likely overstained. Such overstaining not only obscures the fine particulate nature of the desmotubule, but also accentuates open spaces in the cytoplasmic annulus to simulate "negatively stained" or electron-lucent particles. We used only 0.1% tannic acid in our study, and found no increase in the diameter of microfilaments (Ding et al. 1991 c). Therefore, our protocol appears to result in minimal distortion of the native dimensions of cell structures.

On the basis of these considerations, we conclude that the electron-dense particles of plasmodesmata in our study represent positively stained particles, and the electron-lucent areas represent spaces.

Plasmodesmatal substructure

Our observation of particles in the inner leaflet of the plasma membrane of plasmodesmata of tobacco confirms earlier observations made with other plants (Robards 1968, Thomson and Platt-Aloia 1985) and indicates that such particles, probably proteinaceous, are regular structural components of plasmodesmata. Plasmodesmata particles have also been seen in freeze-fracture studies (Willison 1976, Thompson and Platt-Aloia 1985) although the position and size of the particles do not correspond exactly to our interpretation.

We have found that it is difficult to determine the exact number of desmotubule wall particles in a transverse view. This may be due to the oblique orientation of gyres of particles (see below) combined with slight bending in the desmotubule, which can obscure the distinction between particles, or falsely increase the number of particles. Tilting the sections helped clarify, but not completely resolve, some of the obscured particles. Depending on the tilt angle, from seven to ten desmotubule wall particles can be counted. However, a careful analysis of the desmotubule in transverse views indicate that the number of particles is most likely to be seven (see Fig. 3 a–c).

Several other authors (Robards 1968, Zee 1969, Olesen 1979) have described various numbers of electron-lucent subunits for the desmotubule. However, such subunits should not be confused with the electron-dense particles in our micrographs. As discussed above, we interpret the electron-lucent subunits of the desmotubule in previous models (Robards 1968, Zee 1969, Olesen 1979) as open spaces between the positively-stained particles of the desmotubule wall and the plasma membrane. The rotational reinforcement (Markham et al. 1963) micrographs in those papers (Robards 1968, Zee 1969, Olesen 1979) were probably taken from young plasmodesmata without central cavities or from the neck regions of more mature plasmodesmata. Since the desmotubule and the plasma membrane are closely spaced in this region (see Fig. 3 a–c) the open spaces between them could have been reinforced and misinterpreted as electron-lucent particles (Robards 1968, Zee 1969, Olesen 1979). We have used the rotational technique of Markham et al. (1963) to illustrate how the technique can produce "electron lucent particles" from inter-particulate spaces (Fig. 6 b and c). A comparison of our interpretation and that of Olesen and Robards (1990), which incorporates the model of Overall et al. (1982), is given in Fig. 7.

The central rod sometimes appears to be composed of two particles when viewed at certain tilt angles. Because of the relatively close spacing between the two central rod particles observed at some tilt angles, we can exclude the possibility that the second particle is one of the surrounding desmotubule wall particles that is visualized due to tilting. Instead, our interpretation is that a series of particles form the so-called "central rod" within the desmotubule. Thus, when the central rod appears to be a particle in transverse views, we are viewing the central rod straight down from one end (0° tilt relative to the normal transverse plane of the desmotubule). When such a section is tilted, an oblique view of the central rod is obtained and we see two, or perhaps more (if interference of the desmotubule wall particles could be excluded), particles in the center of the desmotubule (see Fig. 3 c). This can be seen most easily if the desmotubule is curved, or if the central rod particles are off-registered slightly along the longitudinal axis; otherwise the desmotubule wall particles interfere with the image. Although we have no clear evidence, we suggest that the center-to-center distance of the central rod particles is similar to that between striations of the desmotubule wall particles. This could explain why a solid central rod is not observed in longitudinal views. In such views it would be impossible to distinguish the particles of the central rod from those of the desmotubule wall.

A recent study combining enzymatic, plasmolytic, and electron microscopic approaches by Tilney et al. (1991) indicates that the desmotubule is largely proteinaceous. This supports our observation of the particulate nature of the desmotubule. However, there is also evidence in the literature to suggest that the desmotubule is composed of fused ER membrane (Gunning and Hughes 1976, Hepler 1982, Overall et al. 1982, Gunning and Hughes 1976, Hepler 1982, Overall et al. 1982, Gunning and Overall 1983, Mollenhauer and Morré 1987). For example, Mollenhauer and Morré (1987) fixed corn root tips with potassium permanganate alone, which mainly preserved lipid but rarely proteins (Millonig and Marinozz 1968), and a compressed ER was seen clearly to traverse the plasmodesmata in the space occupied by the desmotubule. Considering the available data, we conclude that the desmotubule wall is composed of protein particles that are, at least partially, embedded in the outer leaflet of the fused ER membrane. As suggested by Overall et al. (1982), the central rod represents the fused inner leaflets of ER membrane. But in contrast to their conclusion, we suggest that the central rod possibly also contains protein particles, because lipids alone are very unlikely to form particulate structures. Recently, connexin-related proteins have been localized in plasmodesmata (Yahalom et al. 1991). Whether or not the desmotubule particles are such connexin-related proteins needs further investigation.

The protein particles of the desmotubule wall are most likely organized into discrete gyres with nearly uniform spacing and orientation. The gyres have a pitch of 20–30° with reference to the transverse axis of the desmotubule. Viewing sections at various tilt angles does not reveal a helical pattern of particle arrangement (e.g., no criss-cross pattern of particle striations were ever observed). However, a precise determination of particle organization is complicated by factors such as optical superimposition of particles, limited value of stereo pairs at high magnifications, and relative closeness of particles.

Fine filamentous connections between the central rod and the desmotubule wall have been shown before in some chemically fixed tissues (Robards 1968, Zee 1969). Our results confirm these observations. Due to the very narrow dimensions involved, and the unknown precise composition of the central rod, it is difficult to speculate on the chemical nature of these filaments.

The spoke-like structures that extend from the desmotubule to the plasma membrane in the central cavity region of plasmodesmata have also been observed before in chemically fixed tissues (Burgess 1971). Therefore such structures may be a universal feature of central cavities of plasmodesmata. Because of the limited spatial-separation capability of high magnification stereo pairs, it is not easy to determine from single micrographs whether these spoke-like structures interconnect the particles of the desmotubule and the plasma membrane, or whether they extend through the interparticulate gaps of the desmotubule and the plasma membrane. However, in almost all observations, in transverse or longitudinal views, these structures appear to extend from particles to particles. Thus we suggest that the spoke-like structures interconnect particles of the desmotubule and the plasma membrane. We do not know whether these structures are stretched-out remains of originally very short connections between the desmotubule and plasma membrane that might have been present prior to the formation of the central cavity.

We have not found any evidence for the presence of an external sphincter-like structure in or around plasmodesmata of tobacco leaves, in contrast to observations in other studies using different plants (Olesen 1979, Robards 1976, Robards and Lucas 1990, Mollenhauer and Morré 1987). Neither have we observed an internal sphincter-like structure in the neck region of plasmodesmata as Evert et al. (1977) reported in some dicots. Whether the presence of sphincter-like structures is species-dependent, or whether it represents a chemical fixation artifact reinforced by tannic acid overstaining, remains to be determined.

Based on the images that we have obtained and what we consider to be the most convincing evidence in the literature, we propose a model of plasmodesmatal substructure (Fig. 8).

Regulation of plasmodesmatal transport

Our plasmodesmatal model indicates that the open spaces between protein particles of the desmotubule wall and the plasma membrane are the most likely channels for passages of molecules and ions between cells (see Fig. 7 b). The width of these transport channels (2.5 nm) is in close agreement with the calculated diameter of open channels derived from dye coupling experiments with the *Abutilon* nectary trichome (3 nm) (Terry and Robards 1987) and the *Elodea* leaf (3–5 nm) (Goodwin 1983).

An important feature of our model is that the transport channels are interconnected through gaps between gyres of the desmotubule wall particles. Therefore, these channels are not necessarily discrete and straight, but may be tortuous.

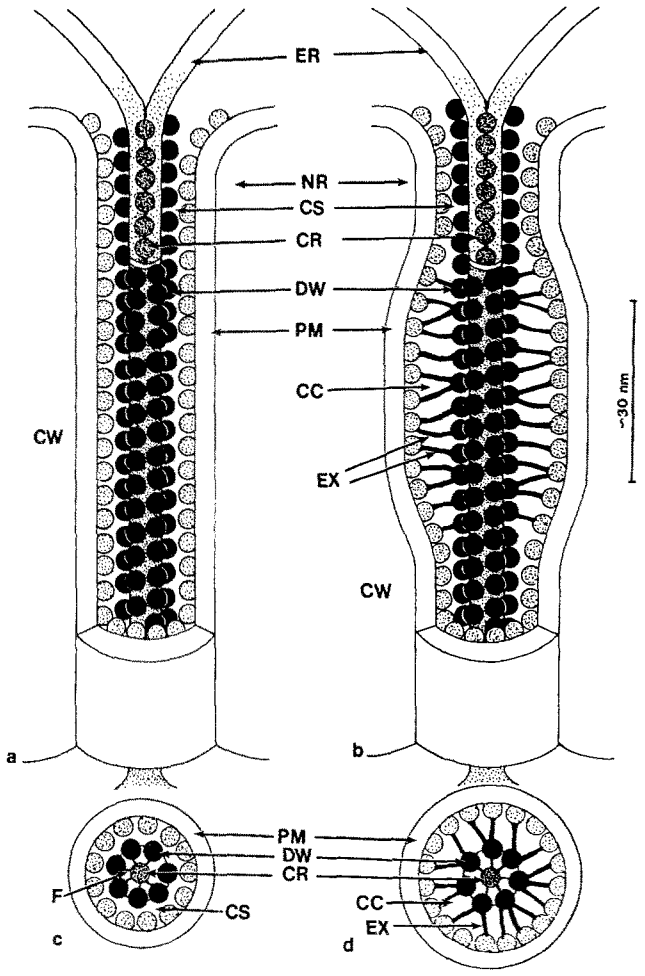

Fig. 8. A model of plasmodesmatal substructure. **a** A plasmodesma with no central cavity. **b** A plasmodesma with central cavity. **c** A transverse view of any region of the plasmodesma shown in **a**, and is also a transverse view of the neck region (*NR*) of the plasmodesma shown in **b**. **d** A transverse view of the central cavity (*CC*) region of the plasmodesma shown in **b**. The desmotubules in **a** and **b** are drawn as a stereo pair. The plasma membrane (*PM*) is continuous through the plasmodesmatal pore between adjacent cells. Electron-dense (proteinaceous) particles are shown partially embedded in the lipid of the inner leaflet of the plasma membrane. However, the degree to which they are embedded cannot be determined by present techniques. That is, we do not know whether they are transmembranous proteins or proteins anchored to one of the leaflets of the lipid layer. The endoplasmic reticulum (*ER*) is connected to the desmotubule. The desmotubule wall (*DW*) is composed of electron-dense, proteinaceous particles that are shown partially embedded in the outer leaflet of the lipid bilayer of the fused ER membrane. These particles are arranged into discrete gyres with with a pitch of 20–30° relative to the transverse axis of the desmotubule. The degree to which the desmotubule wall particles are embedded in the lipid cannot be determined either. The central rod (*CR*) of the desmotubule is depicted as a series of particles, probably proteins, embedded in the lipid of fused inner leaflet of ER membrane. The lipid component does not stain as densely as the protein. *CS* Cytoplasmic sleeve. The membrane details are not depicted so that the particles could be accentuated. In **b** and **d**, spoke-like extensions (*EX*) between the desmotubule and the plasma membrane are indicated. In **c**, filamentous structures (*F*) extending from the central rod to the desmotubule wall are indicated

It has been shown that, theoretically, small changes in pore size drastically change the permeability of nuclear (Paine et al. 1975) and plasmodesmatal pores (Terry and Robards 1987). Based on our model, we suggest that the effective pore size (transport channels) of plasmodesmata is determined and regulated by the relative position of protein particles of the desmotubule and those of the plasma membrane. Ca^{2+} and IP_3 (inositol-trisphosphate) appear to be involved in regulation of plasmodesmatal transport (Erwee and Goodwin 1983; Baron-Epel et al. 1988; Tucker 1988, 1990). Though the mechanisms are still not understood, the protein particles of the desmotubule and/or plasma membrane of plasmodesmata can be the sites of action of Ca^{2+} and IP_3 regulation.

As Overall et al. (1982) have pointed out, the free space within the desmotubule could at most accomodate a few water molecules. However, there is the possibility that some molecules, particularly lipophilic ones, could pass between cells through the membrane continuity of the desmotubule or the plasma membrane (see Baron-Epel et al. 1988).

The regulation of plasmodesmatal transport probably occurs at the neck region of plasmodesmata, as that region maintains the same structural compactness during plasmodesmatal development. The significance of the development of central cavity in terms of plasmodesmatal function remains to be determined.

It must be emphasized that the change in plasmodesmatal pore size that is needed for normal intercellular transport regulation could be too small to be detected by conventional electron microscopic techniques. Therefore, it is not surprising that substantial differences in transport properties can be apparent in plasmodesmata with seemingly identical ultrastructure (Erwee and Goodwin 1983, Palevitz and Hepler 1985).

Acknowledgement

We are grateful for the help of Ms. Carole Daugherty, Ms. Nancy Rizzo, and Ms. Yan Xun. We thank Ms. Bente King for illustrations of the plasmodesmatal models. We also thank Dr. Dwight Beebe, Dr. Roger Spanswick, and Dr. Randy Wayne for helpful discussions and suggestions. This research was supported by grants from the National Science Foundation (DCB 91-04159) and USDA Competetive Grants Program (9000854) to R.T. and NSF Instrumentation grant (BBS-8614106) to M.V.P.

References

Baron-Epel O, Hernandez D, Jiang LW, Meiners S, Schindler M (1988) Dynamic continuity of cytoplasmic and membrane compartments between plant cells. J Cell Biol 106: 715–721

Burgess J (1971) Observations on structure and differentiation in plasmodesmata. Protoplasma 73: 83–95

Calvert HE, Pence MK, Peters GA (1986) Ultrastructural ontogeny of leaf cavity trichomes in *Azolla* implies a functional role in metabolite exchange. Protoplasma 129: 10–27

Ding B, Parthasarathy MV, Niklas K, Turgeon R (1988) A morphometric analysis of the phloem unloading pathway in developing tobacco leaves. Planta 176: 307–318

– Turgeon R, Parthasarathy MV (1991 a) Plasmodesmatal substructure in cryofixed developing tobacco leaf tissue. In: Bonnemain JL, Delrot S, Dainty J, Lucas WJ (eds) Recent advances in phloem transport and assimilate compartmentation. Quest Editions, Nantes, pp 317–323

– – – (1991 b) Routine cryofixation of plant tissues by propane jet freezing for freeze substitution. J Electron Microsc Techn 19: 107–117

– – – (1991 c) Microfilament organization and distribution in freeze substituted tobacco plant tissues. Protoplasma 165: 96–105

Erwee MG, Goodwin PB (1983) Characterization of the *Egeria densa* Planch. leaf symplast. Inhibition of the intercellular movement of fluorescent probes by group II ions. Planta 158: 320–328

Evert RF, Eschrich W, Heyser W (1977) Distribution and structure of plasmodesmata in mesophyll cells of *Zea mays* L. Planta 136: 77–89

Fujiwara K, Link RW (1982) The use of tannic acid in microtubule research. In: Wilson L (ed) Methods in cell biology. Academic Press, New York, pp 217–233

Futaesaku Y, Mizuhira V, Nakamura H (1972) The new fixation method using tannic acid for electron microscopy and some observations of biological specimens. In: Proceedings of the IVth International Congress for Histochemistry and Cytochemistry, pp 155–166

Goodwin PB (1983) Molecular size limit for movement in the symplast of the *Elodea* leaf. Planta 157: 124–130

Gunning BES, Hughes JE (1976) Quantitative assessment of symplastic transport of pre-nectar into the trichomes of *Abutilon* nectaries. Aust J Plant Physiol 3: 619–637

– Overall RL (1983) Plasmodesmata and cell-to-cell transport in plants. BioScience 33: 260–265

– Robards AW (eds) (1976) Intercellular communication in plants: studies on plasmodesmata. Springer, Berlin Heidelberg New York

Hepler PK (1982) Endoplasmic reticulum in the formation of the cell plate and plasmodesmata. Protoplasma 111: 121–133

Lancelle SA, Cresti M, Hepler PK (1987) Ultrastructure of the cytoskeleton in freeze-substituted pollen tubes of *Nicotiana alata*. Protoplasma 140: 141–150

Lopez-Saez JF, Gimenez-Martin G, Risueno MC (1966) Fine structure of the plasmodesm. Protoplasma 61: 81–84

Markham R, Frey S, Hills GJ (1963) Methods for the enhancement of image detail and accentuation of structure in electron microscopy. Virology 20: 88–102

Millonig G, Marinozzi V (1968) Fixation and embedding in electron microscopy. In: Barer R, Cosslett VE (eds) Advances in optical and electron microscopy, vol 2. Academic Press, New York, pp 251–341

Mollenhauer HH, Morré DJ (1987) Some unusual staining properties of tannic acid in plants. Histochemistry 88: 17–22

Olesen P (1979) The neck constriction in plasmodesmata evidence for a peripheral sphincter-like structure revealed by fixation with tannic acid. Planta 144: 349–358

– Robards AW (1990) The neck region of plasmodesmata: general architecture and some functional aspects. In: Robards AW, Jongsma H, Lucas WJ, Pitts J, Spray D (eds) Parallels in cell to cell junctions in plants and animals. Springer, Berlin Heidelberg New York Tokyo, pp 145–170

Overall RL, Wolfe J, Gunning BES (1982) Intercellular communication in *Azolla* roots: I. Ultrastructure of plasmodesmata. Protoplasma 111: 134–150

Paine PL, Moor LC, Horowitz SB (1975) Nuclear envelope permeability. Nature 254: 109–114

Palevitz BA, Hepler PK (1985) Changes in dye coupling of stomatal cells of *Allium* and *Commelina* demonstrated by microinjection of Lucifer Yellow. Planta 164: 473–479

Robards AW (1968) A new interpretation of plasmodesmatal ultrastructure. Planta 82: 200–210

– (1971) The ultrastructure of plasmodesmata. Protoplasma 72: 315–323

– (1976) Plasmodesmata in higher plants. In: Gunning BES, Robards AW (eds) Intercellular communication in plants: studies on plasmodesmata. Springer, Berlin Heidelberg New York, pp 15–57

– Lucas WJ (1990) Plasmodesmata. Annu Rev Plant Physiol Plant Mol Biol 41: 369–419

Scalet M, Crivellato E, Mallardi F (1989) Demonstration of phenolic compounds in plant tissues by an osmium-iodide postfixation procedure. Stain Technol 64: 273–280

Seagull RW, Heath IB (1979) The effect of tannic acid on the in vivo preservation of microfilaments. Eur J Cell Biol 20: 184–188

– – (1980) The differential effects of cytochalasin B on microfilament populations and cytoplasmic streaming. Protoplasma 103: 231–240

Spurr AR (1969) A low viscosity epoxy resin embedding medium for electron microscopy. J Ultrastruct Res 26: 31–43

Terry BR, Robards AW (1987) Hydrodynamic radius alone governs the mobility of molecules through plasmodesmata. Planta 171: 145–157

Thomson WW, Platt-Aloia (1985) The ultrastructure of the plasmodesmata of the salt glands of *Tamarix aphylla* as revealed by transmission electron microscopy and freeze fracture electron microscopy. Protoplasma 125: 13–23

Tilney LG, Bryan J, Bush DJ, Fujiwara K, Mooseker MS, Murphy DB, Snyder DH (1973) Microtubules: evidence for 13 protofilaments. J Cell Biol 59: 267–275

– Cooke TJ, Connelly PS, Tilney MS (1991) The structure of plasmodesmata as revealed by plasmolysis, detergent extraction, and protease digestion. J Cell Biol 122: 73–747

Tiwari SC, Polito VS (1988) Organization of the cytoskeleton in pollen tubes of *Pyrus communis*: a study employing conventional and freeze-substitution electron microscopy, immunofluorescence, and rhodamine-phalloidin. Protoplasma 147: 100–112

– Wick SM, Williamson RE, Gunning BES (1984) Cytoskeleton and integration of cellular function in cells of higher plants. J Cell Biol 99: 63s–69s

Tucker EB (1988) Inositol bisphosphate and inositol triphosphate inhibit cell-to-cell passage of carboxyfluorescein in staminal hairs of *Setcreasea purpurea*. Planta 174: 358–363

– (1990) Calcium-loaded 1,2-bis(2-aminophenoxy)ethane-N,N,N′,N′-tetraacetic acid blocks cell-to-cell diffusion of carboxyfluorescein in staminal hairs of *Setcreasea purpurea*. Planta 82: 34–38

Turgeon R (1984) Termination of nutrient import and development of vein loading capacity of albino tobacco leaves. Plant Physiol 76: 45–48

– (1987) Phloem unloading in tobacco sink leaves: insensitivity to anoxia indicates a symplastic pathway. Planta 171: 73–81

Willison JHM (1976) Plasmodesmata: a freeze fracture view. Can J Bot 54: 2842–2847

Yahalom A, Warmbrodt RD, Laird DW, Traub O, Revel JP, Willecke K, Epel BL (1991) Maize mesocotyl plasmodesmata proteins crossreact with connexin gap junction protein antibodies. Plant Cell 3: 407–417

Zee SY (1969) The fine structure of differentiating sieve elements of *Vicia faba*. Aust J Bot 17: 441–456